

PanGu-Draw: Advancing Resource-Efficient Text-to-Image Synthesis with Time-Decoupled Training and Reusable Coop-Diffusion

Guansong Lu¹ Yuanfan Guo¹ Jianhua Han¹ Minzhe Niu¹ Yihan Zeng¹
 Songcen Xu¹ Zeyi Huang² Zhao Zhong² Wei Zhang¹ Hang Xu¹
¹Huawei Noah’s Ark Lab ²Huawei

Abstract

Current large-scale diffusion models represent a giant leap forward in conditional image synthesis, capable of interpreting diverse cues like text, human poses, and edges. However, their reliance on substantial computational resources and extensive data collection remains a bottleneck. On the other hand, the integration of existing diffusion models, each specialized for different controls and operating in unique latent spaces, poses a challenge due to incompatible image resolutions and latent space embedding structures, hindering their joint use. Addressing these constraints, we present “PanGu-Draw”, a novel latent diffusion model designed for resource-efficient text-to-image synthesis that adeptly accommodates multiple control signals. We first propose a resource-efficient Time-Decoupling Training Strategy, which splits the monolithic text-to-image model into structure and texture generators. Each generator is trained using a regimen that maximizes data utilization and computational efficiency, cutting data preparation by 48% and reducing training resources by 51%. Secondly, we introduce “Coop-Diffusion”, an algorithm that enables the cooperative use of various pre-trained diffusion models with different latent spaces and predefined resolutions within a unified denoising process. This allows for multi-control image synthesis at arbitrary resolutions without the necessity for additional data or retraining. Empirical validations of PanGu-Draw show its exceptional prowess in text-to-image and multi-control image generation, suggesting a promising direction for future model training efficiencies and generation versatility. The largest 5B T2I PanGu-Draw model is released on the Ascend platform. Project page: <https://pangu-draw.github.io>

1. Introduction

The Denoising Diffusion Probabilistic Models (DDPMs) [16] and their subsequent enhancements [6, 15, 29] have established diffusion models as a leading approach for image generation. These advancements excel in the ap-

plication of diffusion models to text-to-image synthesis, yielding high-fidelity results with large-scale models and datasets, supported by substantial computational resources [18, 28, 34, 36, 38]. These foundational models, capable of understanding and rendering complex semantics, have paved the way for diverse image generation tasks, accommodating various control signals such as reference images, edges [51], and poses [51].

However, the extensive computational demand and significant data collection required by these models pose a substantial challenge. The ambitious goal of higher fidelity and increased resolution in image synthesis pushes the boundaries of model and dataset sizes, escalating computational costs, and environmental impact. Moreover, the aspiration for versatile control and multi-resolution in image generation introduces additional complexity. Existing diffusion models, each tailored for specific controls and operating within distinct latent spaces, face the challenge of integration due to incompatible image resolutions and latent space embeddings, obstructing their concurrent utilization. This incompatibility not only leads to more resource consumption of retraining but also impedes the joint synthesis of images controlled by multiple factors, thereby limiting the scalability and practical application of such existing generative models. In response to these challenges, our work introduces a novel paradigm named “PanGu-Draw” that judiciously conserves training resources while enhancing data efficiency, thereby proposing a resource-efficient pathway forward for diffusion model scalability.

As shown in Figure 1, the training strategies of predecessors like DeepFloyd [40] and GLIDE [28], which employ a cascaded approach, excel in leveraging data across resolutions but suffer from inefficient inference due to their reliance on multiple models. Alternatively, Stable Diffusion [36] and AltDiffusion [48] use a Resolution Boost Training strategy aiming for cost-effectiveness by refining a single model. However, this strategy falls short on data efficiency.

In light of these considerations, our PanGu-Draw framework advances the field by presenting a Time-Decoupling Training Strategy that segments the training of a comprehensive text-to-image model into two distinct generators:

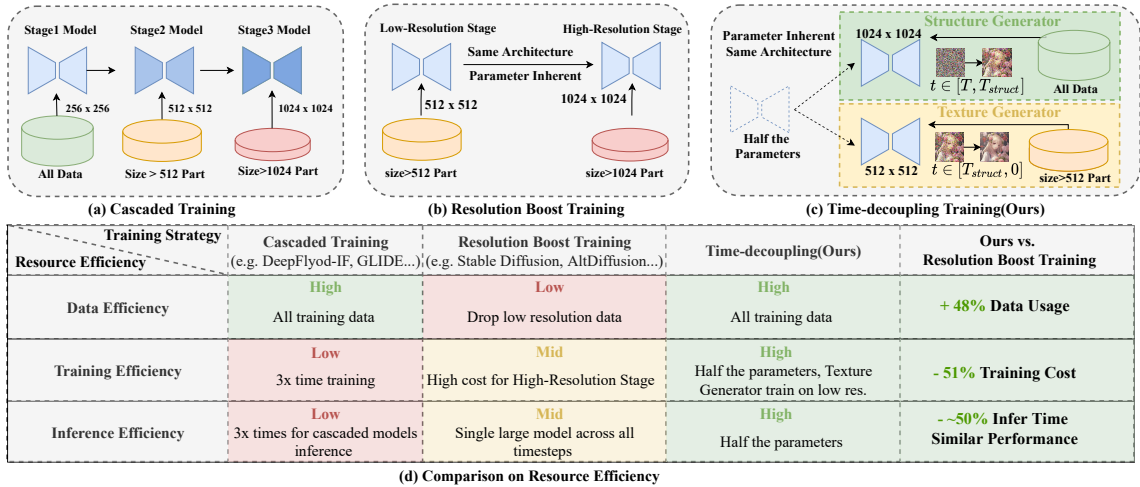


Figure 1. Illustration of three multi-stage training strategies and comparison between them in resource efficiency in data, training and inference aspects. Our time-decoupling training strategy significantly surpasses the representative methods in Cascaded Training [28, 40] and Resolution Boost Training [36, 48] in resource efficiency.

one dedicated to structural outlines and another to textural details. This division not only concentrates on training efforts but also enhances data efficacy. The structural generator is adept at crafting the initial outlines of images, offering flexibility in data quality and enabling training across a spectrum of data calibers; the textural generator, in contrast, is fine-tuned using low-resolution data to infuse these outlines with fine-grained details, ensuring optimal performance even during high-resolution synthesis. This focused approach not only accelerates the training process of our **5B model** but also significantly reduces the reliance on extensive data collection and computational resources, as evidenced by a 48% reduction in data preparation and a 51% reduction in resource consumption.

Furthermore, we introduce a pioneering algorithm named **Coop-Diffusion**, which facilitates the cooperative integration of diverse pre-trained diffusion models. Each model, conditioned on different controls and pre-defined resolutions, contributes to a seamless denoising process. The first algorithmic sub-module addresses inconsistencies in VAE decoders that arise during the denoising process across different latent spaces, ensuring cohesive image quality by effectively reconciling disparate latent space representations. The second sub-module confronts the challenges associated with multi-resolution denoising. Traditional bilinear upsampling for the intermediate noise map, introduced during the denoising process, can undesirably amplify the correlation between pixels. This amplification deviates from the initial Independent and Identically Distributed (IID) assumption, leading to severe artifacts in the final output image. However, our innovative approach circumvents this issue with a single-step sampling method that preserves the integrity of pixel independence, thus preventing the introduction of artifacts. **Coop-Diffusion** obviates the need for additional data or model retraining, addressing

the challenges of multi-control and multi-resolution image generation with scalability and efficiency.

PanGu-Draw excels in text-to-image (T2I) generation, outperforming established models like DALL-E 2 and SDXL, as evidenced by its FID of 7.99 in English T2I. It also leads in Chinese T2I across metrics like FID, IS, and CN-CLIP-score. User feedback highlights a strong preference for PanGu-Draw, aligning well with human visual perceptions. Available on the Ascend platform, PanGu-Draw is efficient and versatile.

In summary, our contributions are manifold:

- **PanGu-Draw**: A resource-efficient diffusion model with a Time-Decoupling Training Strategy, reducing data and training resources for text-to-image synthesis.
- **Coop-Diffusion**: A novel approach for integrating multiple diffusion models, enabling efficient multi-control image synthesis at multi-resolutions within a unified denoising process.
- Comprehensive evaluations demonstrate **PanGu-Draw** (5B model) can produce high-quality images aligned with text and various controls, advancing the scalability and flexibility of diffusion-based image generation.

2. Related Work

Text-to-Image Generation. The integration of diffusion models into the realm of text-to-image generation marks a significant stride in computational creativity [6, 10, 17, 18, 28, 29, 34, 36, 38, 40, 43, 44]. Text-to-image synthesis models like GLIDE [28] and DALL-E 2 [34], which incorporate CLIP image embeddings, have significantly advanced in generating diverse and semantically aligned images from textual descriptions. The Latent Diffusion model [36] addresses computational challenges by creating images from text-conditioned low-dimensional latent representations. Techniques like LoRA [20] enhance domain-specific

adaptability through low-rank matrix-driven parameter offsets, avoiding catastrophic forgetting. Additionally, ControlNet [51] introduces spatial conditioning controls, offering flexibility in image generation under varied conditions like edges and depth. Current research also focuses on aligning model outputs with human aesthetic preferences, aiming to optimize image quality and user satisfaction [8, 13, 23, 41, 42]. Despite the proliferation of such specialized models, a unified framework that consolidates these disparate capabilities remains absent, limiting the potential for multi-control and complex editing in image synthesis.

Model Efficient Training and Scaling Up Strategies. Efficient training and scaling of models are pivotal for advancing large-scale neural networks. In the realm of text-to-image (T2I) diffusion models, the quest for efficiency has led to innovative training strategies. Historical methods, such as those utilized by DeepFloyd [40] and GLIDE [28], capitalize on cascaded approaches that proficiently utilize data across various resolutions, yet their reliance on multiple models results in less efficient inference processes. Contrastingly, models like Stable Diffusion [36] and AltDiffusion [48] adopt Resolution Boost Training strategies that refine a single model for cost-effectiveness. Despite the advantages, such strategies do not fully exploit data efficiency. In scaling up strategies, training efficiency is also important. The correlation between model size and performance is well-documented [19, 22], with larger models like SDXL [30] showing notable gains. Efficient adaptation and scaling are explored in [2] through distillation, and in [31] by marrying model expansion with domain-specific prompts. Serial scaling and knowledge distillation reduce training times significantly as demonstrated by [11], while [7] proposes progressive network expansion for faster training with minimal loss. Our approach offers a novel approach to diffusion model scaling that enhances efficiency.

3. Preliminary

Given an image x_0 , diffusion models first produce a series of noisy images x_1, \dots, x_T by adding Gaussian noise to x_0 according to some noise schedule given by $\bar{\alpha}_t$ as follows:

$$x_t = \sqrt{\bar{\alpha}_t}x_0 + \sqrt{1 - \bar{\alpha}_t}\epsilon, \quad (1)$$

where $\epsilon \sim \mathcal{N}(0, I)$.

Diffusion models then learn a denoising model $\epsilon_\theta(x_t, t)$ to predict the added noise of a noisy image x_t with the following training objective:

$$\mathcal{L} = \mathbb{E}_{x_0 \sim q(x_0), \epsilon \sim \mathcal{N}(0, I), t \sim [1, T]} \|\epsilon - \epsilon_\theta(x_t, t)\|^2, \quad (2)$$

where t is uniformly sampled from $\{1, \dots, T\}$. Once the denoising model $\epsilon_\theta(x_t, t)$ is learned, starting from a random noise $x_T \sim \mathcal{N}(0, I)$, one can iteratively predict and reduce the noise in x_t to get a real image x_0 . During the sampling process, we can predict the clean data x_0 from $\epsilon_\theta(x_t, t)$

with single-step sampling as follows:

$$\hat{x}_{0,t} = \frac{1}{\sqrt{\bar{\alpha}_t}}(x_t - \sqrt{1 - \bar{\alpha}_t}\epsilon_\theta(x_t, t)). \quad (3)$$

Our text-to-image generation model is built on the model architecture proposed in Latent Diffusion Model [36]. In this model, a real image x_0 is first down-sampled 8 times as a lower-dimension latent code z_0 with an image encoder model E , which can be decoded with a latent decoder model D back to a real image x_0 . The denoising network $\epsilon_\theta(z_t, t, c)$ is parameterized as a U-Net [37] model, where embedding of time step t is injected with adaptive normalization layers and embedding of input text c is injected with cross-attention layers.

4. PanGu-Draw

In this section, we first illustrate our resource-efficient 5B text-to-image generation model, trained with a time-decoupling training strategy and further enhanced with a prompt enhancement LLM. Then, we present our *Coop-Diffusion* algorithm for the cooperative integration of diverse pre-trained diffusion models, enabling multi-control and multi-resolution image generation.

4.1. Time-Decoupling Training Strategy

Enhancing data, training, and inference efficiency is vital for text-to-image models’ practical use. Figure 1 shows two existing training strategies: (a) Cascaded Training, using three models to incrementally improve resolution, is data-efficient but triples training and inference time. (b) Resolution Boost Training starts at 512x512 and then 1024x1024 resolution, discarding lower resolution data and offering moderate efficiency with higher training costs and single-model inference across all timesteps. These approaches differ from our time-decoupling strategy, detailed below.

Responding to the need for enhanced efficiencies, we draw inspiration from the denoising trajectory of diffusion processes, where initial denoising stages primarily shape the image’s structural foundation, and later stages refine its textural complexity. With this insight, we introduce the Time-Decoupling Training Strategy. This approach divides a comprehensive text-to-image model, denoted as ϵ_θ , into two specialized sub-models operating across different temporal intervals: a structure generator, ϵ_{struct} , and a texture generator, $\epsilon_{texture}$. Each sub-model is half the size of the original, thus enhancing manageability and reducing computational load.

As illustrated in Figure 1(c), the structure generator, ϵ_{struct} , is responsible for early-stage denoising across larger time steps, specifically within the range T, \dots, T_{struct} , where $0 < T_{struct} < T$. This stage focuses on establishing the foundational outlines of the image. Conversely, the texture generator, $\epsilon_{texture}$, operates during the latter, smaller time steps, denoted by $T_{struct}, \dots, 0$, to

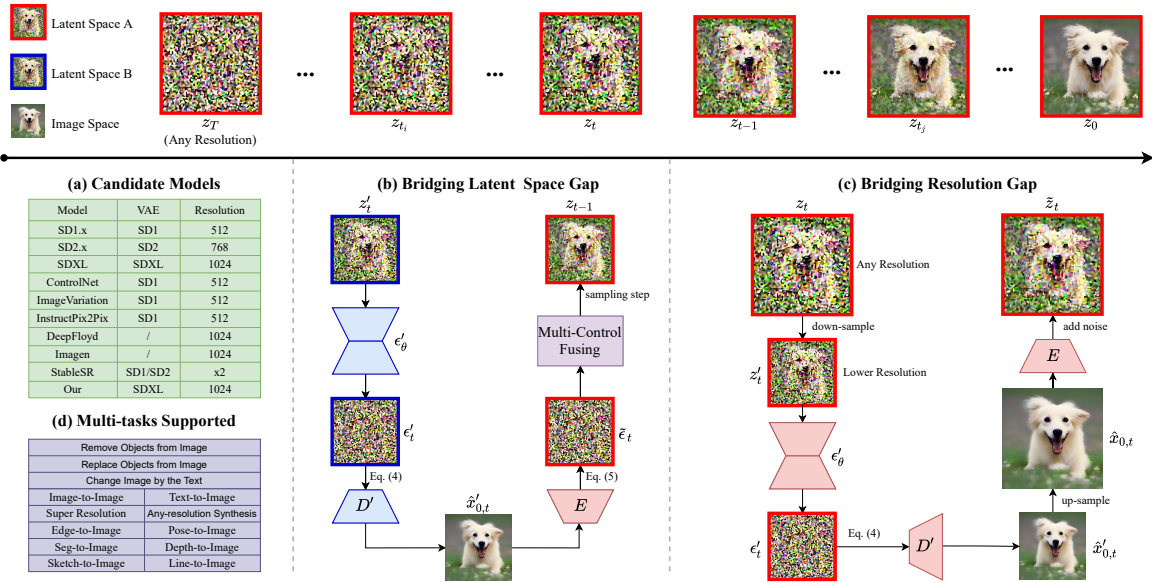


Figure 2. Visualization of our *Coop-Diffusion* algorithm for the cooperative integration of diverse pre-trained diffusion models. (a) Existing pre-trained diffusion models, each tailored for specific controls and operating within distinct latent spaces and image resolutions. (b) This sub-module bridges the gap arising from different latent spaces by transforming ϵ'_t in latent space B to the target latent space A as $\tilde{\epsilon}_t$. (c) This sub-module bridges the gap arising from different resolutions by performing upsampling on the predicted clean data $\hat{x}'_{0,t}$.

elaborate on the textural details. Each generator is trained in isolation, which not only alleviates the need for high-memory computation devices but also avoids the complexities associated with model sharding and its accompanying inter-machine communication overhead.

In the inference phase, ϵ_{struct} initially constructs a base structural image, $z_{T_{struct}}$, from an initial random noise vector, z_T . Subsequently, $\epsilon_{texture}$ refines this base to enhance textural details, culminating in the final output, z_0 . This sequential processing facilitates a more resource-efficient workflow, significantly reducing the hardware footprint and expediting the generation process without compromising the model’s performance or output quality, as demonstrated in our ablated experiment in Sec. 5.3.

Resource-Efficient Specialized Training Regime. We further adopt specialized training designs for the above two models. The structure generator ϵ_{struct} , which derives image structures from text, requires training on an extensive dataset encompassing a wide range of concepts. Traditional methods, like Stable Diffusion, often eliminate low-resolution images, discarding about 48% of training data and thereby inflating dataset costs. Contrarily, we integrate high-resolution images with upscaled lower-resolution ones. This approach, as proven by our ablated experiments in Sec. 5.3, shows no performance drop, as the predicted $z_{T_{struct}}$ still contains substantial noise. In this way, we achieve higher data efficiency and avoid the problem of semantic degeneration.

Additionally, since the image structure is determined in $z_{T_{struct}}$ and the texture generator $\epsilon_{texture}$ focuses on refining texture, we propose training $\epsilon_{texture}$ at a lower resolution while still sampling at high resolution. This strategy, as demonstrated in our ablated experiments in Sec. 5.3, results



Figure 3. Results of fusing a low-resolution model and a high-resolution model with different upsampling methods. Upsampling from intermediate z_t results in severe artifacts, while our upsampling algorithm results in high-fidelity image.

in no performance drop and no structural problems (e.g., repetitive presentation [21]). Consequently, we achieved an overall 51% improvement in training efficiency. Figure 1 summarizes the data, training, and inference efficiency of different training strategies. Besides higher data and training efficiency, our strategy also achieves higher inference efficiency with fewer inference steps compared to the Cascaded Training strategy and a smaller per-step model compared to the Resolution Boost Training strategy.

4.2. Coop-Diffusion: Multi-Diffusion Fusion

As shown in Figure 2(a), there are numerous pre-trained diffusion models, such as various SD, ControlNet, image variation, etc., each tailored for specific controls and image resolutions. It is promising to fuse these pre-trained models for multi-control or multi-resolution image generation without needing to train a new model. However, the different latent spaces and resolutions of these models impede joint synthesis of images controlled by different models, thereby

Algorithm 1 Coop-Diffusion: Multi-Diffusion Fusing

Sub-Module 1. Bridging Latent Space Gap

Input: random noise $z_T \sim \mathcal{N}(0, I)$, diffusion model ϵ_θ , decoder D , encoder E in latent space A; random noise $z'_T = z_T$, diffusion model ϵ'_θ , decoder D' , encoder E' in latent space B; guidance strength d , sampling method S .

```
1: for  $t = T, \dots, 1$  do
2:    $\epsilon'_t = \epsilon'_\theta(z'_t)$ ,  $\hat{z}'_{0,t} = \frac{1}{\sqrt{\alpha_t}}(z'_t - \sqrt{1 - \alpha_t}\epsilon'_t)$ 
3:    $\hat{x}'_{0,t} = D'(\hat{z}'_{0,t})$ ,  $\tilde{z}_{0,t} = E(\hat{x}'_{0,t})$ 
4:    $\tilde{\epsilon}_t = \frac{1}{\sqrt{1 - \alpha_t}}(z_t - \sqrt{\alpha_t}\tilde{z}_{0,t})$ 
5:    $\epsilon_t = \epsilon_\theta(z_t)$ ,  $\epsilon_{t, fuse} = d \cdot \tilde{\epsilon}_t + (1 - d) \cdot \epsilon_t$ 
6:    $z_{t-1} = S(z_t, t, \epsilon_{t, fuse})$ 
7:    $z'_{t-1} = S(z'_t, t, \epsilon'_{t, fuse}) \triangleright \epsilon'_{t, fuse}$  from  $\epsilon_{t, fuse}$  similar to
   the process from  $\epsilon'_t$  to  $\tilde{\epsilon}_t$ , omitted for brevity
8: end for
9: return  $D(z_0)$ 
```

Sub-Module 2. Bridging Resolution Gap

Input: diffusion model ϵ_θ , decoder D , encoder E in high-resolution space; random noise $z'_T \sim \mathcal{N}(0, I)$, diffusion model ϵ'_θ , decoder D' , encoder E' in low-resolution space; low-resolution sampling end step T_{low} , sampling method S .

```
1: for  $t = T, \dots, T_{low} + 1$  do
2:    $\epsilon'_t = \epsilon'_\theta(z'_t)$ ,  $z'_{t-1} = S(z'_t, t, \epsilon'_t)$ 
3: end for
4:  $\hat{z}'_{0, T_{low}} = \frac{1}{\sqrt{\alpha_{T_{low}}}}(z'_{T_{low}} - \sqrt{1 - \alpha_{T_{low}}}\epsilon'_{T_{low}})$ 
5:  $\hat{x}'_{0, T_{low}} = D'(\hat{z}'_{0, T_{low}})$ ,  $\hat{x}_{0, T_{low}} = \text{Upsample}(\hat{x}'_{0, T_{low}})$ 
6:  $\hat{z}_{0, T_{low}} = E(\hat{x}_{0, T_{low}})$ 
7:  $z_{T_{low}} = \sqrt{\alpha_{T_{low}}}\hat{z}_{0, T_{low}} + \sqrt{1 - \alpha_{T_{low}}}\epsilon$ ,  $\epsilon \sim \mathcal{N}(0, I)$ 
8: for  $t = T_{low}, \dots, 1$  do
9:    $\epsilon_t = \epsilon_\theta(z_t)$ ,  $z_{t-1} = S(z_t, t, \epsilon_t)$ 
10: end for
11: return  $D(z_0)$ 
```

limiting their practical applications. In response to these challenges, we propose the *Coop-Diffusion* algorithm with two key sub-modules, as shown in Figures 2(b) and (c), to bridge the latent space gap and the resolution gap, and to unite the denoising process in the same space.

Bridging the Latent Space Gap. To bridge the latent space gap between spaces A and B, we propose to unify the model prediction in latent space A by transforming the model prediction ϵ'_t in latent space B to latent space A using the image space as an intermediate. This is done in the following way: first, we predict the clean data $\hat{z}'_{0,t}$ using Equation (3) as:

$$\hat{z}'_{0,t} = \frac{1}{\sqrt{\alpha_t}}(z'_t - \sqrt{1 - \alpha_t}\epsilon'_t), \quad (4)$$

which is then decoded into a pixel-level image $\hat{x}'_{0,t}$ using the latent decoder model D' . This image is encoded into latent space A using the image encoder model E , as $\tilde{z}_{0,t} = E(\hat{x}'_{0,t})$, and finally transformed into a model prediction by inverting Equation (3) as:

$$\tilde{\epsilon}_t = \frac{1}{\sqrt{1 - \alpha_t}}(z_t - \sqrt{\alpha_t}\tilde{z}_{0,t}). \quad (5)$$

With the united $\tilde{\epsilon}_t$, we can now perform multi-control fusion between $\tilde{\epsilon}_t$ and ϵ_t (the prediction from model ϵ_θ with

Table 1. Comparisons of PanGu-Draw with recent representative English text-to-image generation models on COCO dataset in terms of FID. Our classifier-free guidance scale is set as 2.

Method	FID↓	Model Size	Release
DALL-E [33]	27.50	12B	N
LDM [36]	12.63	1.5B	Y
GLIDE [28]	12.24	5B	N
SDXL [30]	11.93	2.5B	Y
PixArt- α [3]	10.65	0.6B	Y
DALL-E 2 [34]	10.39	5.5B	N
Imagen [38]	7.27	3B	N
RAPHAEL [44]	6.61	3B	N
PanGu-Draw	7.99	5B	Y

z_t in latent space A, omitted in Figure 2 for brevity) as: $\epsilon_{t, fuse} = d \cdot \tilde{\epsilon}_t + (1 - d) \cdot \epsilon_t$, where d and $1 - d$ are the guidance strengths of each model with $d \in [0, 1]$, to guide the denoising process jointly with these two models for multi-control image generation. Algorithm 1 further illustrates this fusion process.

Bridging Resolution Gap. To integrate the denoising processes of a low-resolution model with a high-resolution model, upsampling and/or downsampling is necessary. Traditional bilinear upsampling, often applied to the intermediate result z_t during the denoising process, can undesirably amplify pixel correlation. This amplification deviates from the initial Independent and Identically Distributed (IID) assumption, leading to severe artifacts in the final images, as shown in Figure 3(a). Conversely, downsampling does not present this issue. To address the IID issue in upsampling, we propose a new upsampling algorithm that preserves the IID assumption, thereby bridging the resolution gap between models with different pre-trained resolutions.

Figure 2(c) visualizes our upsampling algorithm. Specifically, for a low-resolution z'_t , we use the image space as an intermediate space to transform z'_t in low-resolution space into high-resolution space as \tilde{z}_t . We first predict the noise ϵ'_t with the denoising model ϵ'_θ and then predict the clean data $\hat{z}'_{0,t}$ as described in Eq. 4. This is decoded into an image $\hat{x}'_{0,t}$ using decoder D' . We then perform upsampling on $\hat{x}'_{0,t}$ to obtain its high-resolution counterpart $\hat{x}_{0,t}$. Finally, $\hat{x}_{0,t}$ is encoded into the latent space with encoder E as $\tilde{z}_{0,t}$, and t -step noise is added to get the final result \tilde{z}_t using Eq. 1.

With the unified \tilde{z}_t , we can now perform multi-resolution fusion. First, we denoise with a low-resolution model to obtain the intermediate z'_t and its high-resolution counterpart \tilde{z}_t . Then, we perform denoising with a high-resolution model starting from \tilde{z}_t , and vice versa. This approach allows us to conduct one-stage super-resolution without undergoing all the low-resolution denoising steps, thereby improving inference efficiency. Algorithm 1 further illustrates this fusion process.



“一位年轻女性，身着优雅礼服，佩戴毕业帽，微笑着面对镜头，伸出手臂，她的背景是夕阳下的校园。” “A young woman, wearing an elegant gown and graduation cap, smiles at the camera and extends her arms, with the sunset on campus in the background.”



“一位面带微笑的女子，身穿白色T恤，红色夹克在阳光下熠熠生辉，画面清新，风格像动漫，细节丰富。” “A smiling woman wearing a white T-shirt and a red jacket shines in the sun. The picture is fresh, anime-like in style, and rich in details.”



“一个巨大的水晶球，内部蕴含着一个微型雨林，雨林中蝴蝶飞舞，阳光透过树叶洒落。” “A huge crystal ball contains a miniature rainforest inside, with butterflies flying in the rainforest and sunlight shining through the leaves.”



“一只穿着中世纪铠甲的兔子，手持长剑站在一座古城堡的城墙上，背后是落日的余晖。” “A rabbit wearing medieval armor and holding a sword stands on the wall of an ancient castle with the setting sun behind him.”



“赛博朋克风格的摄影机，无人机在夜空中飞行，以粒子水墨画风展现，具有强烈的光影效果。” “Cyberpunk style camera, drone flying in the night sky, presented in particle ink painting style, with strong light and shadow effects.”



“旅行者们泛舟在波光粼粼的湖面上，周围是雄伟的山脉，以中国水墨画风格描绘，画面色彩淡雅，具有古典诗意。” “Travelers are boating on the sparkling lake, surrounded by majestic mountains, painted in the style of Chinese ink painting, with elegant colors and a classical poetic feel.”



“一台未来风格的摩托车，闪烁着霓虹灯，停在夜晚的东京街头。” “A futuristic motorcycle, shining with neon lights, is parked on the streets of Tokyo at night.”



“一座由冰晶和雪花构成的精致城堡，坐落在北极的冰原上。” “An exquisite castle made of ice crystals and snowflakes, located on the Arctic ice sheet.”



“一艘古老的海盗船，完全由糖果和巧克力制成。” “An ancient pirate ship made entirely of candy and chocolate.”

Figure 4. Images generated with PanGu-Draw, our 5B multi-lingual text-to-image generation model. PanGu-Draw is able to generate multi-resolution high-fidelity images semantically aligned with the input prompts.

5. Experiments

Implementation Details. We adopt the pretrained Variational Autoencoder (VAE) model from SDXL [30], and we build our structure and texture generator based on the architecture of its U-Net model with the following modifications. To achieve bilingual text-to-image generation (Chinese and English), we pre-train a Chinese text encoder [12, 46] on our Chinese training dataset. We then concatenate the text embeddings from this Chinese text encoder with those from a pretrained English text encoder, serving as the final text embeddings for the denoising models. For multi-resolution image generation, we select a range of image resolutions around 1024x1024 and further condition the denoising model on the sinusoidal positional embeddings corresponding to the index of image resolutions. The T_{struct} parameter is set to 500, as suggested by our ablation study.

Our models are trained on a cluster consisting of 256 Ascend 910B cards. During training, we applied several tech-

niques to reduce redundant memory usage. These include replacing traditional attention with Flash Attention [5], employing mixed-precision training [27], and using gradient checkpointing [4], also known as the recompute technique. These methods enable the model to fit within the memory of a single Neural Processing Unit (NPU), allowing parallelism to be applied only in the data scope and avoiding model sharding among NPUs, as well as reducing inter-machine communication overhead.

Dataset Construction. To encompass the abundant concepts in the world, we collect images in various styles from multiple sources, including Noah-Wukong [12], LAION [35], and others, such as photography, cartoons, portraits, and gaming assets. The collected images are filtered based on CLIP score, aesthetic score, watermark presence, resolution, and aspect ratio. To improve the semantic alignment of PanGu-Draw, we discard parts of the noisy captions that are meaningless or mismatched to the image, sourced from the Internet. Instead, we recaption the collected images by

Table 2. Comparisons of PanGu-Draw with Chinese text-to-image generation models on COCO-CN dataset in terms of FID, IS and CN-CLIP-score. The classifier-free guidance scales are set as 9 following AltDiffusion [48].

Model	FID↓	IS↑	CN-CLIP-score↑
AltDiffusion[48]	25.31	29.16	35.12
Taiyi-Bilingual[50]	24.61	34.29	32.26
Taiyi-CN[50]	23.99	34.29	34.22
PanGu-Draw	21.81	37.00	36.62

Table 3. Results of a User study on ImageVal-prompt in terms of image-text alignment, image fidelity, and aesthetics.

Method	Align↑	Fidelity↑	Aesthetics↑	Ave↑
DALL-E 3[1]	4.72	4.59	4.76	4.69
MJ 5.2	4.63	4.54	4.75	4.64
SDXL[30]	4.41	4.37	4.59	4.46
SD[36]	4.17	3.99	4.20	4.12
PanGu-Draw	4.5	4.52	4.72	4.58

first employing an open-vocabulary detector [47] to locate the primary subjects within the images. These subjects are then processed by LLaVA [26], a high-performance vision-language model, along with prompting templates, to yield detailed image descriptions. These English annotations are subsequently translated into Chinese.

Evaluation Metrics. We evaluate PanGu-Draw’s text-to-image generation on COCO [25] with 30k images for English, and COCO-CN [24] with 10k images for Chinese. The Frechet Inception Distance (FID [14]) is utilized to evaluate image quality and diversity. For Chinese, additional metrics include the Inception Score (IS [39]) and CN-CLIP-score[45], assessing image quality and text-image alignment. Complementing these metrics, a user study is conducted to evaluate image-text alignment, fidelity, and aesthetics using ImageEval-prompt¹ across 339 prompts.

5.1. Text-to-Image Generation

Evaluation on COCO. As shown in Table 1, PanGu-Draw achieves a FID of 7.99, which is superior to compared methods such as DALL-E 2 and SDXL. It also achieves competitive FID with SOTA methods, indicating the effectiveness of our time-decoupling training strategy and its outstanding data and training efficiencies. Our 5B PanGu model is the best-released model in terms of FID.

Evaluation on COCO-CN. As shown in Table 2, PanGu-Draw outperforms other released Chinese text-to-image models, including Taiyi-CN, Taiyi-Bilingual, and AltDiffusion, across all three metrics. This performance highlights PanGu-Draw’s exceptional Chinese text-to-image generation capabilities and the effectiveness of our bilingual text encoder architecture.

User Study. We conducted a user study to compare PanGu-Draw with top-performing methods, including SDXL [30], Midjourney 5.2, and DALL-E 3 [1]. As shown in Table 3, PanGu-Draw achieves better results than SD and

¹<https://github.com/FlagOpen/FlagEval/tree/master/imageEval>

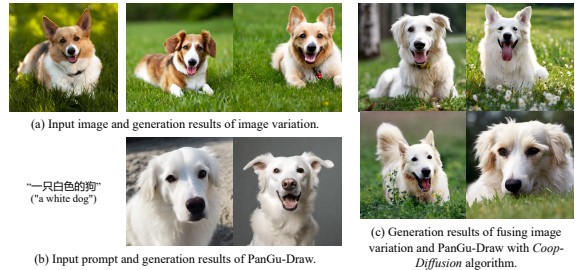


Figure 5. Generation results of the fusing of an image variation model and PanGu-Draw and with the proposed *Coop-Diffusion* algorithm.

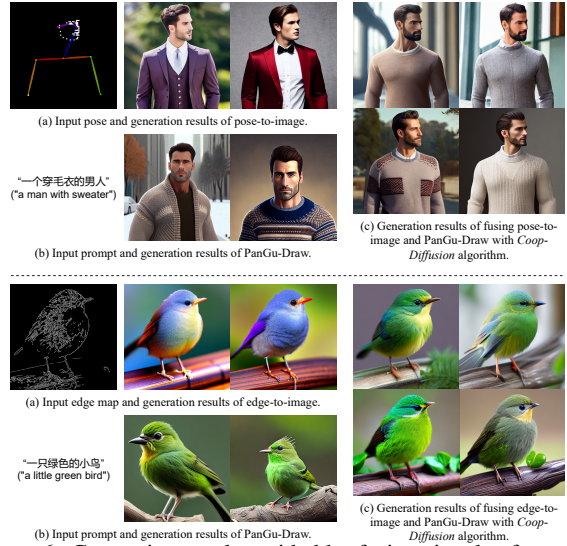


Figure 6. Generation results guided by fusing signals of text and pose/edge map by our *Coop-Diffusion*.

SDXL across all three metrics. It also attains approximately 99%/98% of the performance of Midjourney 5.2 and DALL-E 3, respectively, indicating PanGu-Draw’s excellent text-to-image capabilities. Figure 4 shows a collection of high-fidelity multi-resolution images generated by PanGu-Draw. As we can see, the generated images of PanGu-Draw are of high aesthetics and semantically aligned with the input prompts.

5.2. Multi-Diffusion Fusing Results

Multi-Control Image Generation. To demonstrate the effectiveness of the proposed reusable multi-diffusion fusing algorithm, *Coop-Diffusion*, we first present multiple results of multi-control image generation. Figure 5 displays results from fusing an image variation model² with PanGu-Draw. The fusing results maintain a style similar to that of the reference image, matching the texture described by the input prompt. Figure 6 shows results from fusing PanGu-Draw with a pose/edge-to-image ControlNet model, which operates in guess mode without input prompts. Here, the fusing results combine the structure of the pose/edge image with the texture described by the input prompt.

²<https://huggingface.co/lambdalabs/sd-image-variations-diffusers>



Figure 7. Images generated with a low-resolution (LR) model (first row: text-to-image model; second row: Edge-to-image ControlNet) and the fusion of the LR model and HR PanGu-Draw with our *Coop-Diffusion*. This allows for single-stage super-resolution for better details and higher inference efficiency.

Multi-Resolution Image Generation. We also present multi-resolution image generation results of fusing PanGu-Draw with low-resolution text-to-image and edge-to-image ControlNet model by first denoising with the low-resolution model to get the intermediate z_t and the high-resolution counterpart \tilde{z}_t , and then perform denoising in high resolution with PanGu-Draw. Figure 7 shows the results from the low-resolution model and our fusing algorithm *Coop-Diffusion*. As we can see, PanGu-Draw adds much details to the low-resolution predictions leading to high-fidelity high-resolution results. Besides, compared with the common practice of super-resolution with diffusion model, which carries out all the low-resolution denoising steps, our method achieve higher inference efficiency.

5.3. Ablation Study

In this section, we perform ablation studies to analyze our time-decoupling training strategy. The baseline model has $1B$ parameters while the structure and texture generators both have $0.5B$ parameters. During the training process, the latter two models only train half the steps of the baseline model with T_{struct} set as 500. Both settings of the models are trained from scratch on a subset of the LAION dataset containing images with all sizes. After training, FID, IS and CLIP-score on COCO are reported for comparison.

Time-Decoupling Training Strategy. We compare the final performance of models trained with the Resolution Boost strategy and our time-decoupling strategy in Table 4. We found that models trained with our strategy achieves much better performance in all three criteria, indicating the effectiveness of our strategy.

Training Designs. The structure and texture generators (ϵ_{struct} and $\epsilon_{texture}$) are designed to train on different resolutions to improve data and training efficiency. However,

Table 4. Comparison of models across Resolution Boost (1B parameters) and Time-Decoupling training strategies (0.5B parameters for structure and texture generators)

Model	FID↓	IS↑	CLIP-score↑
Resolution Boost	106.12	10.46	22.9
Time-Decoupling	87.66	11.07	23.4

Table 5. Performance of structure and texture models training with images of different resolutions.

Structure Data	Texture Resolution	FID↓	IS↑	CLIP-score↑
All data	256	87.66	11.07	23.4
Only high resolution	256	89.52	10.96	23.2
All data	512	90.98	10.59	23.3

Table 6. Comparisons of PanGu-Draw inference performance with different time step splitting point T_{struct} settings.

T_{struct}	FID↓	IS↑	CLIP-score↑
200	105.08	10.59	22.98
300	98.08	10.72	23.12
500	87.66	11.07	23.40
700	89.48	11.02	23.32

this approach may negatively influence the final performance. In Table 5, we compare such a design with a traditional training process, where ϵ_{struct} discards low-resolution images, or $\epsilon_{texture}$ trains with high resolution. Results on COCO show that ϵ_{struct} benefits from these extra up-scaled data, and $\epsilon_{texture}$ learns enough texture patterns at a smaller resolution.

Timestep Splitting Point. The timestep splitting point T_{struct} between the structure and texture generators also influences the final performance. To this end, we set T_{struct} to 200, 300, 500, and 700, while keeping the other settings of the structure and texture generators unchanged. As shown in Table 6, as T_{struct} increases from 200 to 700, the performance initially increases and then decreases continuously. $T_{struct} = 500$ is the optimal value, and we adopt it as the default setting in all other experiments.

6. Conclusion

In this paper, we present ‘‘PanGu-Draw’’, a new latent diffusion model for efficient text-to-image generation that effectively integrates multiple control signals. Our approach includes a Time-Decoupling Training Strategy to separate the text-to-image process into structure and texture generation, enhancing data use and computational efficiency. Additionally, ‘‘Coop-Diffusion’’ is introduced, an algorithm allowing cooperative use of different pre-trained diffusion models in a unified denoising process for multi-control image synthesis at various resolutions without extra data or retraining. PanGu-Draw outperforms models like DALL-E 2 and SDXL in English T2I, achieves superior FID, IS, and CN-CLIP-scores in Chinese T2I, and receives favorable user feedback. This positions PanGu-Draw as a versatile and efficient state-of-the-art method, which is available on the Ascend platform.

References

- [1] James Betker, Gabriel Goh, Li Jing, Tim Brooks, Jianfeng Wang, Linjie Li, Long Ouyang, Juntang Zhuang, Joyce Lee, Yufei Guo, et al. Improving image generation with better captions. *Computer Science*. <https://cdn.openai.com/papers/dall-e-3.pdf>, 2023. 7
- [2] Cheng Chen, Yichun Yin, Lifeng Shang, Xin Jiang, Yujia Qin, Fengyu Wang, Zhi Wang, Xiao Chen, Zhiyuan Liu, and Qun Liu. bert2bert: Towards reusable pretrained language models. *arXiv preprint arXiv:2110.07143*, 2021. 3
- [3] Junsong Chen, Jincheng Yu, Chongjian Ge, Lewei Yao, Enze Xie, Yue Wu, Zhongdao Wang, James Kwok, Ping Luo, Huchuan Lu, and Zhenguo Li. Pixart- α : Fast training of diffusion transformer for photorealistic text-to-image synthesis, 2023. 5, 2, 6
- [4] Tianqi Chen, Bing Xu, Chiyuan Zhang, and Carlos Guestrin. Training deep nets with sublinear memory cost, 2016. 6
- [5] Tri Dao, Daniel Y. Fu, Stefano Ermon, Atri Rudra, and Christopher Ré. Flashattention: Fast and memory-efficient exact attention with io-awareness, 2022. 6
- [6] Prafulla Dhariwal and Alexander Nichol. Diffusion models beat gans on image synthesis. *Advances in Neural Information Processing Systems*, 34:8780–8794, 2021. 1, 2
- [7] Ning Ding, Yehui Tang, Kai Han, Chao Xu, and Yunhe Wang. Network expansion for practical training acceleration. In *Proceedings of the IEEE/CVF Conference on Computer Vision and Pattern Recognition*, pages 20269–20279, 2023. 3
- [8] Hanze Dong, Wei Xiong, Deepanshu Goyal, Rui Pan, Shizhe Diao, Jipeng Zhang, Kashun Shum, and Tong Zhang. Raft: Reward ranked finetuning for generative foundation model alignment. *arXiv preprint arXiv:2304.06767*, 2023. 3, 1, 2
- [9] Zhengxiao Du, Yujie Qian, Xiao Liu, Ming Ding, Jiezhong Qiu, Zhilin Yang, and Jie Tang. Glm: General language model pretraining with autoregressive blank infilling. In *Proceedings of the 60th Annual Meeting of the Association for Computational Linguistics (Volume 1: Long Papers)*, pages 320–335, 2022. 1
- [10] Zhida Feng, Zhenyu Zhang, Xintong Yu, Yewei Fang, Lanxin Li, Xuyi Chen, Yuxiang Lu, Jiayang Liu, Weichong Yin, Shikun Feng, et al. Ernie-vilg 2.0: Improving text-to-image diffusion model with knowledge-enhanced mixture-of-denoising-experts. In *Proceedings of the IEEE/CVF Conference on Computer Vision and Pattern Recognition*, pages 10135–10145, 2023. 2, 5, 6
- [11] Cheng Fu, Hanxian Huang, Zixuan Jiang, Yun Ni, Lifeng Nai, Gang Wu, Liqun Cheng, Yanqi Zhou, Sheng Li, Andrew Li, et al. Triple: Revisiting pretrained model reuse and progressive learning for efficient vision transformer scaling and searching. In *ICCV*, 2023. 3
- [12] Jiayi Gu, Xiaojun Meng, Guansong Lu, Lu Hou, Niu Minzhe, Xiaodan Liang, Lewei Yao, Runhui Huang, Wei Zhang, Xin Jiang, et al. Wukong: A 100 million large-scale chinese cross-modal pre-training benchmark. *Advances in Neural Information Processing Systems*, 35:26418–26431, 2022. 6
- [13] Yaru Hao, Zewen Chi, Li Dong, and Furu Wei. Optimizing prompts for text-to-image generation. *arXiv preprint arXiv:2212.09611*, 2022. 3
- [14] Martin Heusel, Hubert Ramsauer, Thomas Unterthiner, Bernhard Nessler, and Sepp Hochreiter. Gans trained by a two time-scale update rule converge to a local nash equilibrium. *Advances in neural information processing systems*, 30, 2017. 7
- [15] Jonathan Ho and Tim Salimans. Classifier-free diffusion guidance. *arXiv preprint arXiv:2207.12598*, 2022. 1
- [16] Jonathan Ho, Ajay Jain, and Pieter Abbeel. Denoising diffusion probabilistic models. *Advances in Neural Information Processing Systems*, 33:6840–6851, 2020. 1
- [17] Jonathan Ho, Ajay Jain, and Pieter Abbeel. Denoising diffusion probabilistic models. *Advances in Neural Information Processing Systems*, 33:6840–6851, 2020. 2
- [18] Jonathan Ho, Chitwan Saharia, William Chan, David J Fleet, Mohammad Norouzi, and Tim Salimans. Cascaded diffusion models for high fidelity image generation. *J. Mach. Learn. Res.*, 23:47–1, 2022. 1, 2
- [19] Jordan Hoffmann, Sebastian Borgeaud, Arthur Mensch, Elena Buchatskaya, Trevor Cai, Eliza Rutherford, Diego de Las Casas, Lisa Anne Hendricks, Johannes Welbl, Aidan Clark, et al. Training compute-optimal large language models. *arXiv preprint arXiv:2203.15556*, 2022. 3
- [20] Edward J Hu, Yelong Shen, Phillip Wallis, Zeyuan Allen-Zhu, Yuanzhi Li, Shean Wang, Lu Wang, and Weizhu Chen. Lora: Low-rank adaptation of large language models. *arXiv preprint arXiv:2106.09685*, 2021. 2, 1
- [21] Zhiyu Jin, Xuli Shen, Bin Li, and Xiangyang Xue. Training-free diffusion model adaptation for variable-sized text-to-image synthesis. *arXiv preprint arXiv:2306.08645*, 2023. 4
- [22] Jared Kaplan, Sam McCandlish, Tom Henighan, Tom B Brown, Benjamin Chess, Rewon Child, Scott Gray, Alec Radford, Jeffrey Wu, and Dario Amodei. Scaling laws for neural language models. *arXiv preprint arXiv:2001.08361*, 2020. 3
- [23] Kimin Lee, Hao Liu, Moonkyung Ryu, Olivia Watkins, Yuqing Du, Craig Boutilier, Pieter Abbeel, Mohammad Ghavamzadeh, and Shixiang Shane Gu. Aligning text-to-image models using human feedback. *arXiv preprint arXiv:2302.12192*, 2023. 3
- [24] Xirong Li, Chaoxi Xu, Xiaoxu Wang, Weiyu Lan, Zhengxiong Jia, Gang Yang, and Jieping Xu. Coco-cn for cross-lingual image tagging, captioning, and retrieval. *IEEE Transactions on Multimedia*, 21(9):2347–2360, 2019. 7
- [25] Tsung-Yi Lin, Michael Maire, Serge Belongie, James Hays, Pietro Perona, Deva Ramanan, Piotr Dollár, and C Lawrence Zitnick. Microsoft coco: Common objects in context. In *Computer Vision—ECCV 2014: 13th European Conference, Zurich, Switzerland, September 6–12, 2014, Proceedings, Part V 13*, pages 740–755. Springer, 2014. 7
- [26] Haotian Liu, Chunyuan Li, Qingyang Wu, and Yong Jae Lee. Visual instruction tuning. *arXiv preprint arXiv:2304.08485*, 2023. 7
- [27] Paulius Micikevicius, Sharan Narang, Jonah Alben, Gregory Diamos, Erich Elsen, David Garcia, Boris Ginsburg, Michael Houston, Oleksii Kuchaiev, Ganesh Venkatesh, and Hao Wu. Mixed precision training, 2018. 6

- [28] Alex Nichol, Prafulla Dhariwal, Aditya Ramesh, Pranav Shyam, Pamela Mishkin, Bob McGrew, Ilya Sutskever, and Mark Chen. Glide: Towards photorealistic image generation and editing with text-guided diffusion models. *arXiv preprint arXiv:2112.10741*, 2021. 1, 2, 3, 5
- [29] Alexander Quinn Nichol and Prafulla Dhariwal. Improved denoising diffusion probabilistic models. In *ICML*, pages 8162–8171. PMLR, 2021. 1, 2
- [30] Dustin Podell, Zion English, Kyle Lacey, Andreas Blattmann, Tim Dockhorn, Jonas Müller, Joe Penna, and Robin Rombach. Sdxl: improving latent diffusion models for high-resolution image synthesis. *arXiv preprint arXiv:2307.01952*, 2023. 3, 5, 6, 7, 2
- [31] Yujia Qin, Jiajie Zhang, Yankai Lin, Zhiyuan Liu, Peng Li, Maosong Sun, and Jie Zhou. Elle: Efficient life-long pre-training for emerging data. *arXiv preprint arXiv:2203.06311*, 2022. 3
- [32] Alec Radford, Jong Wook Kim, Chris Hallacy, Aditya Ramesh, Gabriel Goh, Sandhini Agarwal, Girish Sastry, Amanda Askell, Pamela Mishkin, Jack Clark, et al. Learning transferable visual models from natural language supervision. In *International conference on machine learning*, pages 8748–8763. PMLR, 2021. 1
- [33] Aditya Ramesh, Mikhail Pavlov, Gabriel Goh, Scott Gray, Chelsea Voss, Alec Radford, Mark Chen, and Ilya Sutskever. Zero-shot text-to-image generation. In *International Conference on Machine Learning*, pages 8821–8831. PMLR, 2021. 5
- [34] Aditya Ramesh, Prafulla Dhariwal, Alex Nichol, Casey Chu, and Mark Chen. Hierarchical text-conditional image generation with clip latents. *arXiv preprint arXiv:2204.06125*, 2022. 1, 2, 5, 6
- [35] Robin Rombach, Andreas Blattmann, Dominik Lorenz, Patrick Esser, and Björn Ommer. High-resolution image synthesis with latent diffusion models. In *Proceedings of the IEEE/CVF conference on computer vision and pattern recognition*, pages 10684–10695, 2022. 6
- [36] Robin Rombach, Andreas Blattmann, Dominik Lorenz, Patrick Esser, and Björn Ommer. High-resolution image synthesis with latent diffusion models. In *Proceedings of the IEEE/CVF Conference on Computer Vision and Pattern Recognition (CVPR)*, pages 10684–10695, 2022. 1, 2, 3, 5, 7
- [37] Olaf Ronneberger, Philipp Fischer, and Thomas Brox. U-net: Convolutional networks for biomedical image segmentation. In *Medical Image Computing and Computer-Assisted Intervention—MICCAI 2015: 18th International Conference, Munich, Germany, October 5-9, 2015, Proceedings, Part III 18*, pages 234–241. Springer, 2015. 3
- [38] Chitwan Saharia, William Chan, Saurabh Saxena, Lala Li, Jay Whang, Emily L Denton, Kamyar Ghasemipour, Raphael Gontijo Lopes, Burcu Karagol Ayan, Tim Salimans, et al. Photorealistic text-to-image diffusion models with deep language understanding. *Advances in Neural Information Processing Systems*, 35:36479–36494, 2022. 1, 2, 5
- [39] Tim Salimans, Ian Goodfellow, Wojciech Zaremba, Vicki Cheung, Alec Radford, and Xi Chen. Improved techniques for training gans. *Advances in neural information processing systems*, 29:2234–2242, 2016. 7
- [40] Alex Shonenkov, Misha Konstantinov, Daria Bakshandaeva, Christoph Schuhmann, Ksenia Ivanova, and Nadiia Klokova. Deepfloyd if: A powerful text-to-image model that can smartly integrate text into images, 2023. Online; accessed 16-November-2023. 1, 2, 3, 5, 6
- [41] Xiaoshi Wu, Keqiang Sun, Feng Zhu, Rui Zhao, and Hongsheng Li. Better aligning text-to-image models with human preference. *arXiv preprint arXiv:2303.14420*, 2023. 3
- [42] Jiazheng Xu, Xiao Liu, Yuchen Wu, Yuxuan Tong, Qinkai Li, Ming Ding, Jie Tang, and Yuxiao Dong. Imagereward: Learning and evaluating human preferences for text-to-image generation, 2023. 3
- [43] Xingqian Xu, Zhangyang Wang, Eric Zhang, Kai Wang, and Humphrey Shi. Versatile diffusion: Text, images and variations all in one diffusion model. *arXiv preprint arXiv:2211.08332*, 2022. 2
- [44] Zeyue Xue, Guanglu Song, Qiushan Guo, Boxiao Liu, Zhuofan Zong, Yu Liu, and Ping Luo. Raphael: Text-to-image generation via large mixture of diffusion paths. *arXiv preprint arXiv:2305.18295*, 2023. 2, 5, 6
- [45] An Yang, Junshu Pan, Junyang Lin, Rui Men, Yichang Zhang, Jingren Zhou, and Chang Zhou. Chinese clip: Contrastive vision-language pretraining in chinese. *arXiv preprint arXiv:2211.01335*, 2022. 7
- [46] Lewei Yao, Runhui Huang, Lu Hou, Guansong Lu, Minzhe Niu, Hang Xu, Xiaodan Liang, Zhenguo Li, Xin Jiang, and Chunjing Xu. Filip: Fine-grained interactive language-image pre-training. *arXiv preprint arXiv:2111.07783*, 2021. 6
- [47] Lewei Yao, Jianhua Han, Xiaodan Liang, Dan Xu, Wei Zhang, Zhenguo Li, and Hang Xu. Detclipv2: Scalable open-vocabulary object detection pre-training via word-region alignment. In *Proceedings of the IEEE/CVF Conference on Computer Vision and Pattern Recognition*, pages 23497–23506, 2023. 7
- [48] Fulong Ye, Guang Liu, Xinya Wu, and Ledell Wu. Altdiffusion: A multilingual text-to-image diffusion model, 2023. 1, 2, 3, 7
- [49] Aohan Zeng, Xiao Liu, Zhengxiao Du, Zihan Wang, Hanyu Lai, Ming Ding, Zhuoyi Yang, Yifan Xu, Wendi Zheng, Xiao Xia, et al. Glm-130b: An open bilingual pre-trained model. *arXiv preprint arXiv:2210.02414*, 2022. 1
- [50] Jiaxing Zhang, Ruyi Gan, Junjie Wang, Yuxiang Zhang, Lin Zhang, Ping Yang, Xinyu Gao, Ziwei Wu, Xiaoqun Dong, Junqing He, Jianheng Zhuo, Qi Yang, Yongfeng Huang, Xiayu Li, Yanghan Wu, Junyu Lu, Xinyu Zhu, Weifeng Chen, Ting Han, Kunhao Pan, Rui Wang, Hao Wang, Xiaojun Wu, Zhongshen Zeng, and Chongpei Chen. Fengshenbang 1.0: Being the foundation of chinese cognitive intelligence. *CoRR*, abs/2209.02970, 2022. 7
- [51] Lvmin Zhang, Anyi Rao, and Maneesh Agrawala. Adding conditional control to text-to-image diffusion models. In *Proceedings of the IEEE/CVF International Conference on Computer Vision*, pages 3836–3847, 2023. 1, 3, 2

PanGu-Draw: Advancing Resource-Efficient Text-to-Image Synthesis with Time-Decoupled Training and Reusable Coop-Diffusion

Supplementary Material

7. More Details about PanGu-Draw

Prompt Enhancement LLM with RLAIIF Algorithm. To further enhance our generation quality, we harness the advanced comprehension abilities of large language models (LLM)[9, 49] to align users’ succinct inputs with the detailed inputs required by the model. Specifically, shown in Figure 10, we first construct a human-annotated dataset that enriches succinct prompts with background and style descriptions and then fine-tune the LLM to adapt a succinct prompt to an enriched one using this data. To better adapt to the inputs required by PanGu-Draw, we perform further refinement based on the Reward rAnked FineTuning (RAFT)[8] method. Subsequently, we use the fine-tuned LLM to expand on multiple texts, which are then input into PanGu-Draw for image generation. The best expansions are selected jointly by an aesthetic scoring model³ and a CLIP [32] semantic similarity calculation model, allowing for further fine-tuning of the LLM.

Figure 8 shows the generation results of PanGu-Draw without and with prompt enhancement. As we can see, prompt enhancement serves to add more details and illustration to the original brief prompts, leading to better image aesthetics and semantic alignment.

Controllable Stylized Text-to-Image Generation. While techniques like LoRA [20] allow one to adapt a text-to-image model to a specific style (e.g., cartoon style, human-aesthetic-preferred style), they do not allow one to adjust the degree of the desired style. To this end, inspired by the classifier-free guidance mechanism, we propose to perform controllable stylized text-to-image generation by first construct a dataset consisting of human-aesthetic-prefer, cartoon and other samples with a pretrained human aesthetic scoring model and a cartoon image classification models, and then train the text-to-image generation model with these three kinds of samples. For human-aesthetic-prefer and cartoon samples, we prepend a special prefix to the original prompt, denoted as c_{aes} and $c_{cartoon}$ respectively. During sampling, we extrapolated the prediction in the direction of $\epsilon_{\theta}(z_t, t, c_{style})$ and away from $\epsilon_{\theta}(z_t, t, c)$ as follows:

$$\hat{\epsilon}_{\theta}(z_t, t, c) = \epsilon_{\theta}(z_t, t, \emptyset) + s \cdot (\epsilon_{\theta}(z_t, t, c) - \epsilon_{\theta}(z_t, t, \emptyset)) + s_{style} \cdot (\epsilon_{\theta}(z_t, t, c_{style}) - \epsilon_{\theta}(z_t, t, c)),$$

where s is the classifier-free guidance scale, $c_{style} \in \{c_{aes}, c_{cartoon}\}$ and s_{style} is the style guidance scale.

Figure 9 shows the controllable stylized text-to-image



Figure 8. Text-to-image generation results without and with prompt enhancement. Enriched text improve image generation by better image aesthetic perception (left), more detailed background (middle) and better interpretation of abstract concepts (right).

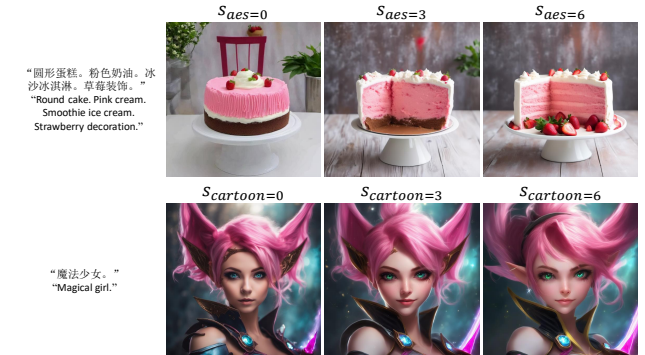


Figure 9. Controllable stylized text-to-image generation results of PanGu-Draw. PanGu-Draw can control the generated images towards the desired style with the style guidance scale. s_{aes} for human-aesthetic-prefer style and $s_{cartoon}$ for cartoon style.

generation results of PanGu-Draw, including human-aesthetic-prefer and cartoon style image generation. As we can see, with the corresponding style guidance scale, PanGu-Draw can control the generated images towards the desired style.

³<https://github.com/christophschuhmann/improved-aesthetic-predictor>

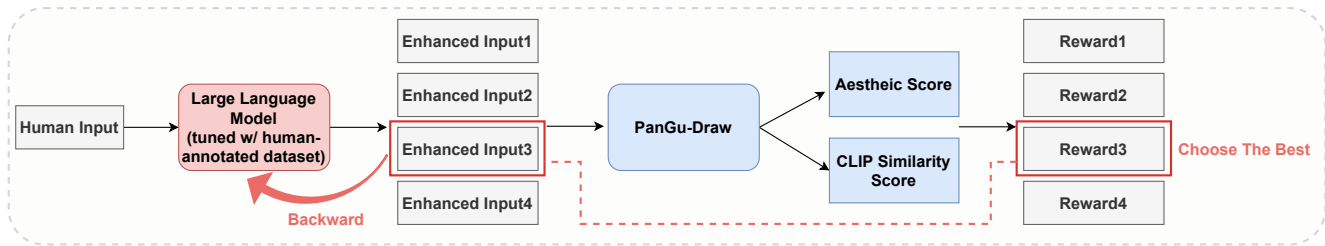


Figure 10. Prompt enhancement pipeline with Large Language Model (LLM), specifically tailored for PanGu-Draw. Initially, we fine-tune the LLM using a human-annotated dataset, transforming a succinct prompt into a more enriched version. Subsequently, to optimize for PanGu-Draw, we employ the Reward rAnked FineTuning (RAFT) method, as introduced in [8], which selects the prompt pairs yielding the highest reward for further fine-tuning.

Table 7. The image resolutions used for multi-resolution training of structure generation model and texture generation model.

Structure Generation Model		Texture Generation Model	
Height	Width	Height	Width
512	2048	256	1024
512	1920	256	960
704	1408	384	768
768	1344	416	736
864	1152	480	640
1024	1024	512	512
1152	864	640	480
1344	768	736	416
1408	704	768	384
1920	512	960	256
2048	512	1024	256

8. Image Resolutions for Multi-Resolution Training

Table 7 shows the list of resolutions used for multi-resolution training of our structure generation model and texture generation model.

9. More Generation Results of PanGu-Draw

9.1. Text-to-Image Generation

Figure 11 shows more generated images of PanGu-Draw. As we can see, the generated images are of high visual quality and are well aligned with the input prompts.

9.2. Multi-Diffusion Fusing Results

Multi-Control Image Generation. Figure 12 shows results of multi-control image generation by fusing PanGu-Draw with different models, including image variation, depth-to-image, edge-to-image generation models.

Figure 13 shows results of fusing two ControlNet models with our algorithm and with the algorithm proposed by ControlNet [51], which fuses the features of different Con-

trolNets before injecting into the U-Net model. As we can see, our algorithm is able to specify the prompts of different ControlNets such that enabling a finer-grain control.

Multi-Resolution Image Generation. Figure 14 shows the results from the low-resolution model and our fusing algorithm *Coop-Diffusion* by fusing the low-resolution model and our high-resolution PanGu-Draw model. As we can see, PanGu-Draw adds much details to the low-resolution predictions leading to high-fidelity high-resolution results.

10. Visual Comparison against Baselines

Figure 15 and 16 shows qualitative comparisons of PanGu-Draw against baseline methods, including RAPHAEL [44], SDXL [30], DeepFloyd [40], DALL-E 2 [34], ERNIE-ViLG 2.0 [10], PixArt- α [3] and . The input prompts are also used in RAPHAEL and are provided at the bottom of the figure. As we can see, PanGu-Draw generates high-quality images, which are better than or on par with these top-performing models.



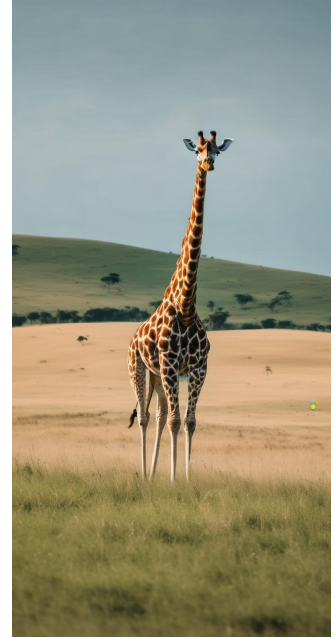
“唐朝美少女，真人，甜美可爱，高清摄影，细节清晰，紫色的长发在阳光下熠熠生辉，微笑的面容，色彩鲜艳。” “Beautiful girl from the Tang Dynasty, real person, sweet and cute, high-definition photography, clear details, long purple hair shining in the sun, smiling face, bright colors.”



“喵喵帽的绿色花朵，洛丽塔风格的摄影，色彩鲜明，光影自然。” “Green flowers in Meow Hat, Lolita style photography, bright colors, natural light and shadow.”



“一只精致的陶瓷猫咪雕像，全身绘有精美的传统花纹，眼睛仿佛会发光。” “An exquisite ceramic cat statue with exquisite traditional patterns painted all over its body and eyes that seem to glow.”



“一只悠然自得的长颈鹿在绿色草原上悠闲地行走。” “A carefree giraffe walks leisurely on the green grassland.”



“极具真实感的复杂的老人肖像。” “Realistically complex portrait of an elderly person.”



“超大广角下，沙漠、河流、绿洲交相辉映，落日余晖洒满大地，此景宛如摄影艺术家的作品，画面开阔，色彩丰富。” “Under the super wide angle, deserts, rivers, and oasis complement each other, and the setting sun fills the earth. This scene is like the work of a photography artist, with a broad picture and rich colors.”



“动漫风格的风景画，有山脉、湖泊，也有繁华的小镇，色彩鲜艳，光影效果明显。” “Animation-style landscape paintings, including mountains, lakes, and bustling towns, with bright colors and obvious light and shadow effects.”



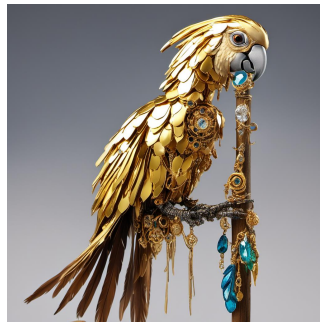
“一项装饰有各种热带鸟类羽毛的华丽帽子。” “An ornate hat decorated with feathers from various tropical birds.”



“一只色彩斑斓的鹦鹉，栖息在繁花似锦的树枝上，画面风格为写实摄影，光影下鹦鹉毛发纹理清晰可见。” “A colorful parrot is perched on a branch full of flowers. The style of the picture is realistic photography. The texture of the parrot's hair is clearly visible under the light and shadow.”



“一幅科幻风格的宇航员照片，背景为星空，人物左右对称，蓝光照亮全身，照片清晰，色彩鲜明，以纸艺和生物发光效果呈现。” “A sci-fi style photo of an astronaut with a starry sky in the background. The figure is symmetrical. Blue light illuminates the whole body. The photo is clear and colorful. It is presented with paper art and bioluminescence effects.”



“一只金色的机械鹦鹉，它的羽毛由闪亮的金属片组成，眼睛像宝石一样闪耀，站在一根古老航海木杆上。” “A golden mechanical parrot, its feathers made of shiny metal flakes and its eyes shining like gems, stands on an ancient nautical wooden pole.”



“金色猴子身着机甲，身姿娇小可爱，具有强烈的武侠元素，居中展现。采用电影特效和粒子特效，光线追踪，呈现出8K画质和极佳的细节刻画。” “The golden monkey is dressed in a mecha, petite and cute, with strong martial arts elements, shown in the center. It uses movie special effects, particle special effects, and ray tracing to present 8K image quality and excellent detail characterization.”

Figure 11. Images generated with PanGu-Draw, our 5B multi-lingual text-to-image generation model. PanGu-Draw is able to generate multi-resolution high-fidelity images semantically aligned with the input prompts.

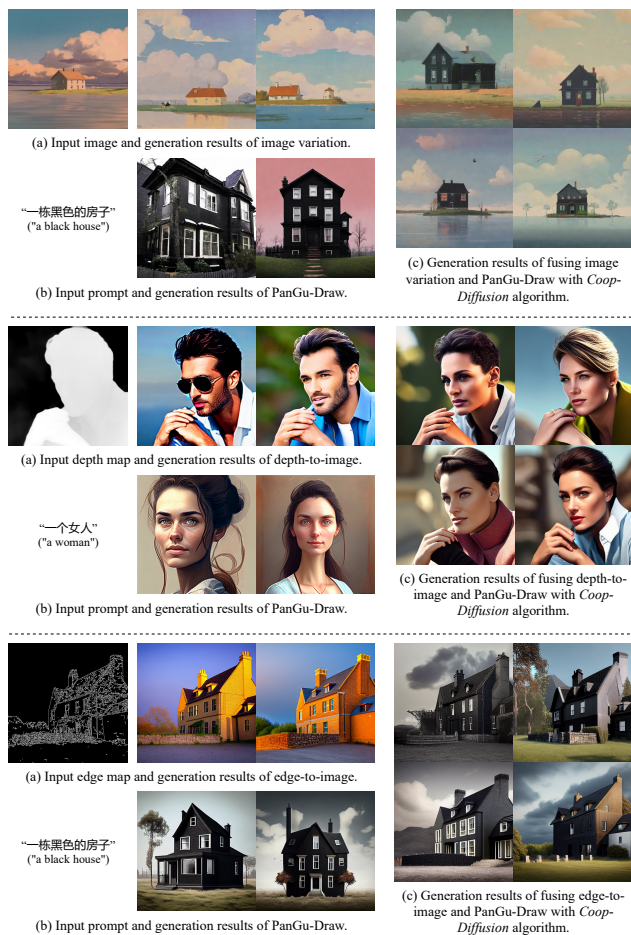


Figure 12. Generation results of the fusion of an image variation/depth-to-image/edge-to-image model and PanGu-Draw with the proposed *Coop-Diffusion* algorithm.

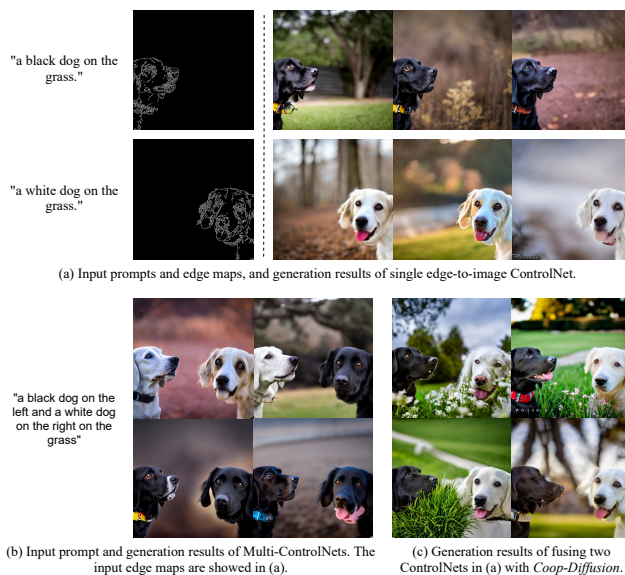
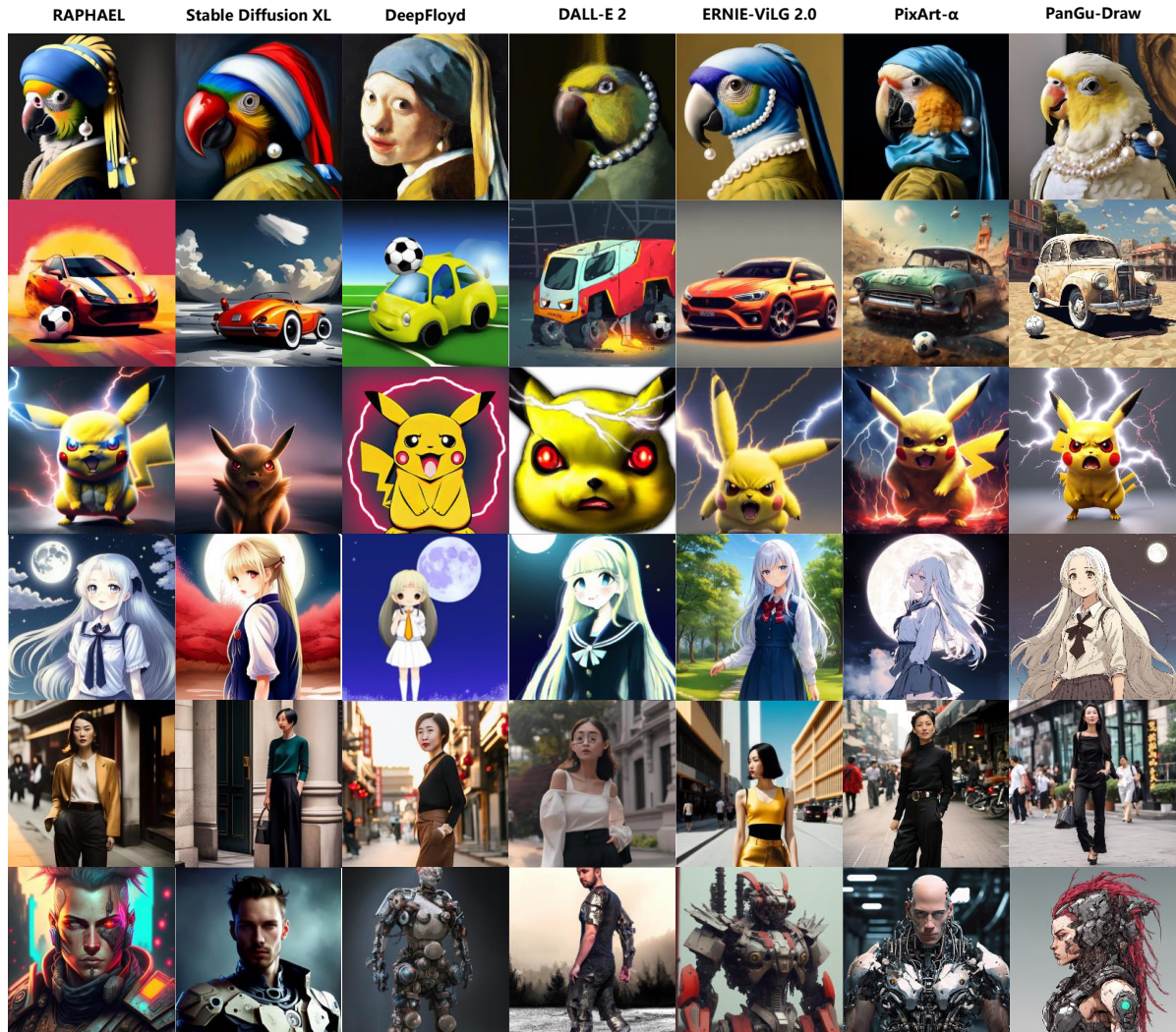


Figure 13. Generation results of the fusion of an image variation/depth-to-image/edge-to-image model and PanGu-Draw with the proposed *Coop-Diffusion* algorithm.

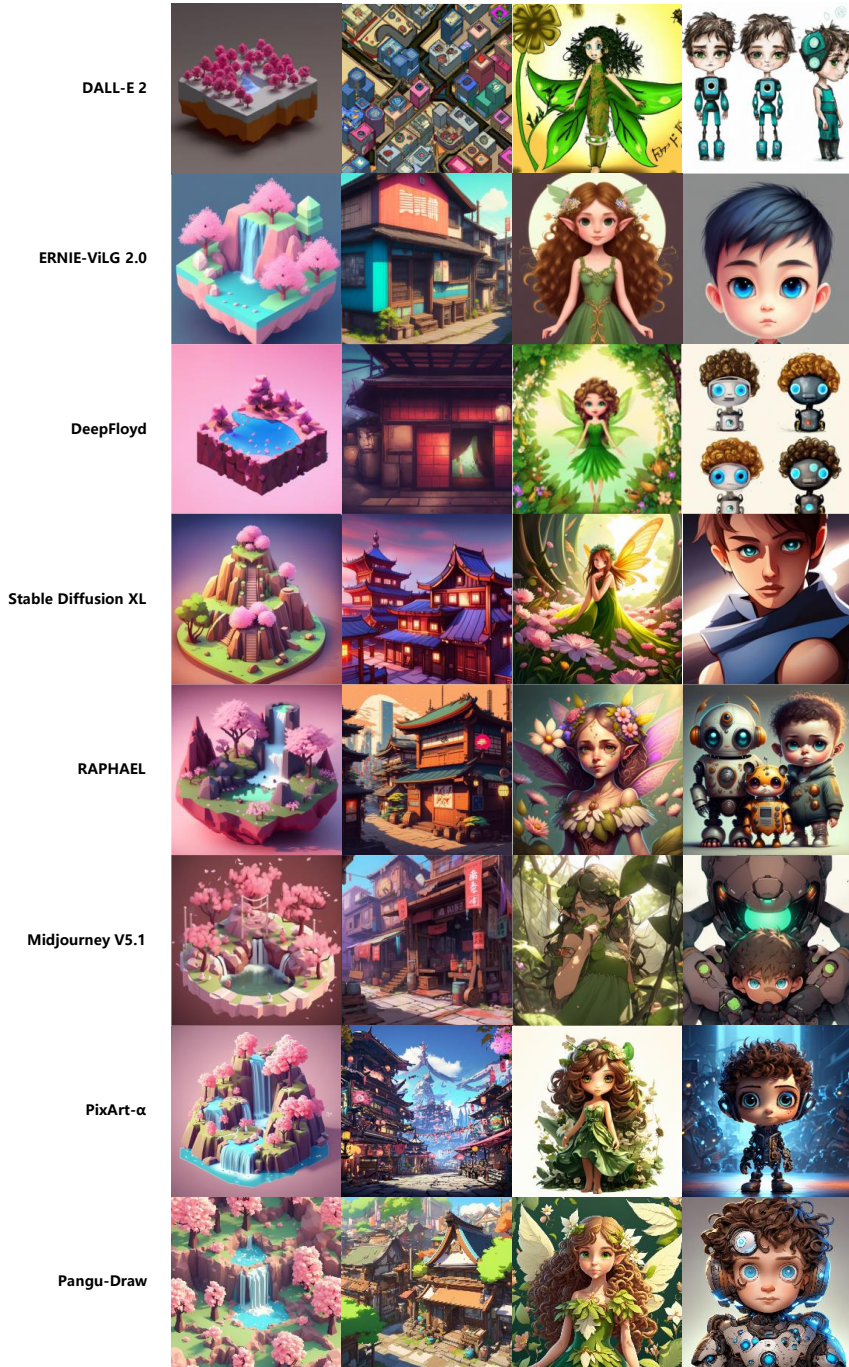


Figure 14. Images generated with a low-resolution (LR) model and the fusion of the LR model and HR PanGu-Draw with our *Coop-Diffusion*. This allows for single-stage super-resolution for better details and higher inference efficiency.



1. A parrot with a pearl earring, Vermeer style.
2. A car playing soccer, digital art.
3. A Pikachu with an angry expression and red eyes, with lightning around it, hyper realistic style.
4. Moonlight Maiden, cute girl in school uniform, long white hair, standing under the moon, celluloid style, Japanese manga style.
5. Street shot of a fashionable Chinese lady in Shanghai, wearing black high-waisted trousers.
6. Half human, half robot, repaired human, human flesh warrior, mech display, man in mech, cyberpunk.

Figure 15. Visual comparison of PanGu-Draw against baseline methods, including RAPHAEL [44], SDXL [30], DeepFloyd [40], DALL-E 2 [34], ERNIE-ViLG 2.0 [10], and PixArt- α [3]. The input prompts are also used in RAPHAEL and are provided at the bottom of the figure. The results of PanGu-Draw are better than or on par with these top-performing baseline models.



1. A cute little matte low poly isometric cherry blossom forest island, waterfalls, lighting, soft shadows, trending on Artstation, 3d render, monument valley, fez video game.
2. A shanty version of Tokyo, new rustic style, bold colors with all colors palette, video game, genshin, tribe, fantasy, overwatch.
3. Cartoon characters, mini characters, figures, illustrations, flower fairy, green dress, brown hair, curly long hair, elf-like wings, many flowers and leaves, natural scenery, golden eyes, detailed light and shadow , a high degree of detail.
4. Cartoon characters, mini characters, hand-made, illustrations, robot kids, color expressions, boy, short brown hair, curly hair, blue eyes, technological age, cyberpunk, big eyes, cute, mini, detailed light and shadow, high detail.

Figure 16. Visual comparison of PanGu-Draw against baseline methods, including DALL-E 2 [34], ERNIE-ViLG 2.0 [10], DeepFloyd [40], SDXL [30], RAPHAEL [44], Midjourney V5.1 and PixArt-α [3]. The input prompts are also used in RAPHAEL and are provided at the bottom of the figure. The results of PanGu-Draw are better than or on par with these top-performing baseline models.